Inorg. Chem. **2007**, *46*, 3557–3565

Energy Decomposition Analysis of Metal–Metal Bonding in $[M_2X_8]^{2-}$ (X = Cl, Br) Complexes of 5f (U, Np, Pu), 5d (W, Re, Os), and 4d (Mo, Tc, Ru) Elements

Germán Cavigliasso[†] and Nikolas Kaltsoyannis*[,‡]

Department of Chemistry, Faculty of Science, Australian National University, Canberra ACT 0200, Australia, and Department of Chemistry, University College London, 20 Gordon Street, London WC1H 0AJ, United Kingdom

Received December 6, 2006

The electronic structures of a series of $[M_2X_8]^{2-}$ (X = Cl, Br) complexes involving 5f (U, Np, Pu), 5d (W, Re, Os), and 4d (Mo, Tc, Ru) elements have been calculated using density functional theory, and an energy decomposition approach has been used to carry out a detailed analysis of the metal–metal interactions. The energy decomposition analysis involves contributions from orbital interactions (mixing of occupied and unoccupied orbitals), electrostatic effects (Coulombic attraction and repulsion), and Pauli repulsion (associated with four-electron two-orbital interactions). As previously observed for Mo, W, and U M_2X_6 species, the general results suggest that the overall metal–metal interaction is considerably weaker or unfavorable in the actinide systems relative to the d-block analogues, as a consequence of a significantly more destabilizing contribution from the combined Pauli and electrostatic (prerelaxation) effects. Although the orbital-mixing (postrelaxation) contribution to the total bonding energy is predicted to be larger in the actinide complexes, this is not sufficiently strong to compensate for the comparatively greater destabilization originating from the Pauli-plus-electrostatic effects. A generally weak electrostatic contribution accounts for the large prerelaxation destabilization in the f-block systems, and ultimately for the weak or unfavorable nature of metal–metal bonding between the actinide elements. There is a greater variation in the energy decomposition results across the $[M_2Cl_8]^{2-}$ series for the actinide than for the d-block elements, both in the general behavior and in some particular properties.

1. Introduction

The synthesis of actinide species with unsupported metal−metal bonds has proved extremely difficult and remains something of a "Holy Grail" in actinide chemistry, with successful attempts limited to matrix-isolated species, for example, the uranium hydrides with U_2H_2 and U_2H_4 chemical compositions.[1] Given the experimental difficulties in making molecular compounds containing actinide−actinide bonds and, therefore, the paucity of such species, computational chemistry plays a particularly valuable role in the investigation and understanding of metal−metal bonding involving 5f elements.[2−8]

In a recent publication,[9] we reported the results of density functional calculations on a series of model uranium, tungsten, and molybdenum M_2X_6 (X = Cl, F, OH, NH_2, CH_3) species. These calculations indicated that multiple ($\sigma + 2\pi$) bonds are formed between the metal atoms in all species investigated, with the orbital properties of these metal−metal bonds corresponding to predominant d−d character in the Mo and W complexes and f−f character in the U systems. Using an energy decomposition approach, the overall metal−

* To whom correspondence should be addressed. E-mail: n.kaltsoyannis@ucl.ac.uk.
[†] Australian National University.
[‡] University College London.

(1) Souter, P. F.; Kushto, G. P.; Andrews, L.; Neurock, M. *J. Am. Chem. Soc.* **1997**, *119*, 1682.
(2) Pepper, M.; Bursten, B. E. *J. Am. Chem. Soc.* **1990**, *112*, 7803.
(3) (a) Gagliardi, L.; Roos, B. O. *Nature* **2005**, *433*, 848. (b) Roos, B. O.; Malmqvist, P. A.; Gagliardi, L. *J. Am. Chem. Soc.* **2006**, *128*, 17000.
(4) Archibong, E. F.; Ray, A. K. *Phys. Rev. A: At., Mol., Opt. Phys.* **1999**, *60*, 5105.
(5) Straka, M.; Pyykkö, P. *J. Am. Chem. Soc*. **2005**, *127*, 13090.
(6) Cayton, R. H.; Novo-Gradac, K. J.; Bursten, B. E. *Inorg. Chem.* **1991**, *30*, 2265.
(7) Roos, B. O.; Gagliardi, L. *Inorg. Chem.* **2006**, *45*, 803.
(8) La Macchia, G.; Brynda, M.; Gagliardi, L. *Angew. Chem., Int. Ed.* **2006**, *45*, 6210.
(9) Cavigliasso, G.; Kaltsoyannis, N. *Inorg. Chem*. **2006**, *45*, 6828.

10.1021/ic0623260 CCC: $37.00
Published on Web 03/24/2007

Chart 1

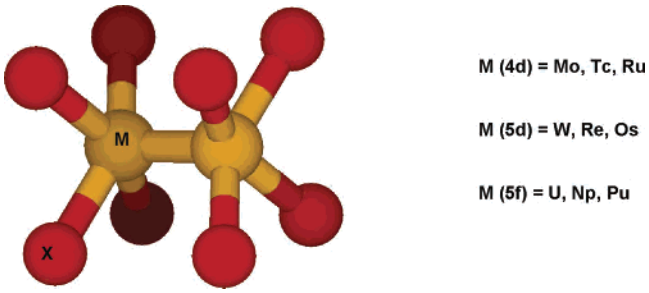

Table 1. Calculated Metal−Metal Distances for the Eclipsed (D_{4h}) Conformations of $[M_2X_8]^{2-}$ Complexes

metal	ligand	M−M (pm)	metal	ligand	M−M (pm)
Mo	Cl	228	Np	Cl	220
	Br	228		Br	220
W	Cl	234	Ru	Cl	221
	Br	235		Br	222
U	Cl	235	Os	Cl	226
	Br	235		Br	227
Tc	Cl	217	Pu	Cl	208
	Br	218		Br	208
Re	Cl	224			
	Br	224			

metal bond strength was calculated to be substantially greater in the Mo and W species than in the U analogues. Although the orbital-mixing interactions are stronger in the U complexes, the relative weakness of U−U bond is a consequence of the significantly more destabilizing nature of the combined Pauli repulsion and electrostatic interaction, suggesting that there are intrinsic intramolecular reasons as to why metal−metal bonding is so scarce in the 5f block.

We have also recently completed comparative density functional and multiconfigurational (ab initio) investigations on a series of model $[M_2X_8]^{2-}$ (X = Cl, Br, I) complexes involving 5f (U, Np, Pu), 5d (W, Re, Os), and 4d (Mo, Tc, Ru) elements.[10] These studies focused on the description and analysis of trends in the electronic structures and metal−metal interactions across the d-block and f-block series. They revealed interesting similarities and differences in the most significant structural and bonding characteristics of the $[M_2X_8]^{2-}$ systems, between both the actinides and d-block elements and also the eclipsed (D_{4h}) and staggered (D_{4d}) conformations of these species.

In this article, we concentrate on the energetics of the metal−metal interactions in these $[M_2X_8]^{2-}$ complexes and present a detailed energy decomposition analysis of the (D_{4h}) Cl and Br species (Chart 1). Our aim is to build on the primarily qualitative study given in our previous paper[10] by providing a quantitative description and rationalization of the general trends in electronic structure and metal−metal bonding across the 5f, 5d, and 4d target systems. As the early-to-middle part of the 5f series is crossed, the radial extension of the 5f orbitals decreases, and the chemistry of the actinides begins to tend toward more lanthanide-like behavior. Thus, it might be expected that significant changes will occur in chemical behavior and properties across the (U, Np, Pu) series (potentially larger than across d-block series involving elements from groups 6, 7, and 8). The existence and nature of such changes are a focus of this contribution.

2. Computational Details

All density functional calculations reported in this article were carried out with the Amsterdam Density Functional (ADF 2004) package.[11−13] A generalized-gradient-approximation functional consisting of the exchange expression proposed by Handy and Cohen[14] and the correlation expression proposed by Perdew, Burke, and Ernzerhof,[15] labeled OPBE, was utilized.

This choice of density functional was based on tests carried out on several M_2X_6 and $[M_2X_8]^{2-}$ complexes,[9,10] for which experimental data are available.

Basis sets of triple-ζ quality and one polarization function (TZP or type IV), incorporating frozen cores (Cl.2p, Br.3d, I.4d and M.3d, M.4f, M.5d for the 4d, 5d, and 5f metal series, respectively), were employed.[11−13] This choice of frozen cores implies that the "outer core plus valence" regions of the metal atom basis sets are comparable or equivalent in character and size. Relativistic effects were included by means of the zero-order regular approximation.[16−18] Plots of the molecular orbitals were generated with the MOLEKEL program[19,20] using data in MOLDEN format[21,22] derived from the ADF TAPE21 files.

3. Results and Discussion

A detailed description and analysis of the molecular and electronic structures of $[M_2X_8]^{2-}$ (X = Cl, Br, I) complexes of 5f (U, Np, Pu), 5d (W, Re, Os), and 4d (Mo, Tc, Ru) elements have been presented in a previous publication.[10] The most relevant results, in the context of the energy decomposition analysis reported in this work, are summarized in Table 1 and Chart 2, which contain the calculated metal−metal distances and show the most significant aspects of the metal−metal interactions, respectively.

For the Mo, W, and U complexes, the individual metal-based configurations are d^3 or f^3, and a formal triple bond, which can be characterized as $[\sigma + 2\pi]$, is therefore possible. For the remaining complexes, in addition to the $[\sigma + 2\pi]$ interactions, the δ orbitals must also be taken into consideration. Consequently, the formal metal−metal bond orders

(10) Cavigliasso, G.; Kaltsoyannis, N. *Dalton Trans*. **2006**, 5476.

(11) *ADF, SCM, Theoretical Chemistry*; Vrije Universiteit: Amsterdam, The Netherlands. http://www.scm.com.
(12) Fonseca Guerra, C.; Snijders, J. G.; te Velde, G.; Baerends, E. J. *Theor. Chem. Acc*. **1998**, *99*, 391.
(13) te Velde, G.; Bickelhaupt, F. M.; van Gisbergen, S. J. A.; Fonseca Guerra, C.; Baerends, E. J.; Snijders, J. G.; Ziegler, T. *J. Comput. Chem*. **2001**, *22*, 931.
(14) Handy, N. C.; Cohen, A. J. *Mol. Phys*. **2001**, *99*, 403.
(15) Perdew, J. P.; Burke, K.; Ernzerhof, M. *Phys. Rev. Lett*. **1996**, *77*, 3865.
(16) van Lenthe, E.; Baerends, E. J.; Snijders, J. G. *J. Chem. Phys*. **1993**, *99*, 4597.
(17) van Lenthe, E.; Baerends, E. J.; Snijders, J. G. *J. Chem. Phys*. **1994**, *101*, 9783.
(18) van Lenthe, E.; Ehlers, A. E.; Baerends, E. J. *J. Chem. Phys*. **1999**, *110*, 8943.
(19) *MOLEKEL: An Interactive Molecular Graphics Tool*; Swiss National Supercomputing Centre. http://www.cscs.ch/molekel/.
(20) Portmann, S.; Lüthi, H. P. *Chimia* **2000**, *54*, 766.
(21) Schaftenaar, G.; Noordik, J. H. *MOLDEN: A Pre- and Post-Processing Program for Molecular and Electronic Structures*, 2000. http://www.cmbi.ru.nl/molden/molden.html.
(22) Schaftenaar, G.; Noordik, J. H. *J. Comput.-Aided Mol. Design* **2000**, *14*, 123.

Chart 2

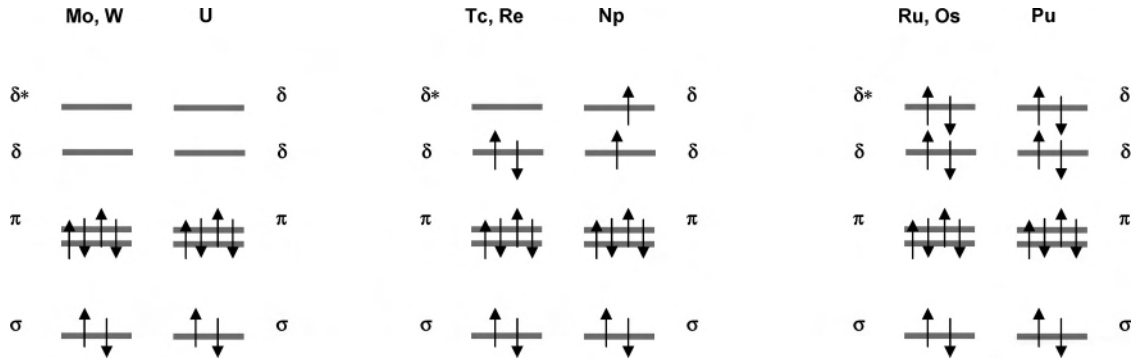

can vary between 3.0 and 5.0, depending on the individual metal-based configurations (d^4, d^5, f^4, f^5) and the bonding, nonbonding, or antibonding character of the δ-like interactions.

In the d-block systems, two primary metal−metal δ orbitals occur as a bonding and antibonding combination in D_{4h} symmetry. For the Ru and Os complexes, these two δ orbitals are fully occupied and thus make no formal contribution to metal−metal bonding. Therefore, analogous to the case of the Mo, W, and U species, a formal ($\sigma + 2\pi$) triple bond is predicted. Only two electrons can reside in the δ orbitals in the Tc and Re complexes, resulting in a fully occupied bonding level and a $[\sigma^2\pi^4\delta(\uparrow\downarrow)^2]$ singlet configuration. Although a formal metal−metal bond order of 4.0 could be assigned to this configuration, the results from both multiconfigurational and density functional calculations suggest that the δ-like interaction is rather weak and that the Tc−Tc and Re−Re bond order should be considered closer to 3.0 than 4.0.[10,23,24]

Unlike the d-block case, in the actinide complexes both δ orbitals possess bonding character, leading to formal metal−metal bond orders of 4.0 and 5.0 for the Np and Pu species, respectively, as a consequence of their occupation by two or four electrons. The Pu complexes are characterized by a singlet configuration, corresponding to the $[\sigma^2\pi^4\delta^4]$ occupation pattern, but for the Np systems, the triplet $[\sigma^2\pi^4\delta(\uparrow)^1\delta(\uparrow)^1]$ configuration is predicted to be somewhat more stable than the singlet $[\sigma^2\pi^4\delta(\uparrow\downarrow)^2]$ configuration.

3.1. Energy Decomposition Analysis. An analysis of bonding energetics[25,26] can be performed by combining a fragment approach to the molecular structure of a chemical system with the decomposition of the total bonding energy (E_B) as

$$E_B = E_E + E_P + E_O \qquad (1)$$

where E_E, E_P, and E_O are, respectively, the electrostatic interaction, Pauli repulsion, and orbital-mixing terms. A detailed description of the physical significance of these properties has been given by Bickelhaupt and Baerends.[27]

The bonding energy (E_B) can be considered a measure of the "instantaneous" interactions between the fragments in the molecule but does not represent the bond dissociation energy (E_D), which is defined as

$$E_D = E_B + E_F \qquad (2)$$

and contains, in addition to the bonding energy, a contribution (E_F) arising from the fragment preparation processes, which can be described as the energy associated with the fragments' transformation from their equilibrium geometry and electronic state into their "intrinsic" geometric and electronic state in the molecule.

The electrostatic component is calculated from the superposition of the unperturbed fragment densities at the molecular geometry and corresponds to the classical electrostatic effects associated with Coulombic attraction and repulsion. The electrostatic contribution is most commonly dominated by the nucleus−electron attractions and therefore has a stabilizing influence.

The Pauli component is obtained by requiring that the electronic antisymmetry conditions be satisfied and has a destabilizing character, whereas the orbital-mixing component represents a stabilizing factor originating from the relaxation of the molecular system due to the mixing of occupied and unoccupied orbitals and can involve electron-pair bonding, charge-transfer or donor−acceptor interactions, and polarization.

3.1.1. General Bonding Energy Results. The fragments used in the energy decomposition analysis can take any chemical form, including single atoms and ions, and neutral or charged molecular units. In addition, several electronic states may be possible and plausible for the separated fragments.

In the present work, the fragment chemical and electronic structures have been chosen so that they correspond, as closely as possible, to the multiple bonding environment in the (D_{4h}) $[M_2X_8]^{2-}$ molecular system. Thus, the most natural "fragmentation" scheme for the analysis of the metal−metal interactions in these complexes is

$$[X_4M(n\uparrow)]^- + [MX_4(n\downarrow)]^- \leftrightarrow [M_2X_8]^{2-} \qquad (3)$$

where the $[MX_4]^-$ fragments possess ideal C_{4v} symmetry and

(23) Gagliardi, L.; Roos, B. O. *Inorg. Chem.* **2003**, *42*, 1599.
(24) Saito, K.; Nakao, Y.; Sato, H.; Sakaki, S. *J. Phys. Chem. A* **2006**, *110*, 9710.
(25) Ziegler, T.; Rauk, A. *Inorg. Chem.* **1979**, *18*, 1558.
(26) Ziegler, T.; Rauk, A. *Inorg. Chem.* **1979**, *18*, 1755.
(27) Bickelhaupt, F. M.; Baerends, E. J. *Rev. Comput. Chem.* **2000**, *15*, 1.

Table 2. Energy Decomposition Analysis of $[M_2Cl_8]^{2-}$ Complexes[a]

metal	E_B	$E_P + E_E$	E_P	E_E	E_O	E_O (a_1)	E_O (a_2)	E_O (b_1)	E_O (b_2)	E_O (e)
Mo	−0.82	6.66	13.08	−6.42	−7.48	−2.94	0.00	−0.05	−0.03	−4.45
W	−1.83	6.07	16.12	−10.05	−7.90	−3.02	0.00	−0.05	−0.02	−4.80
U	−0.05	11.37	11.89	−0.52	−11.42	−3.41	0.00	−0.11	−0.01	−7.89
Tc	0.04	7.73	12.80	−5.07	−7.69	−3.33	0.00	−0.08	0.26	−4.53
Re	−1.39	7.28	16.25	−8.97	−8.66	−3.66	0.00	−0.06	0.14	−5.08
Np	1.23	14.90	16.54	−1.64	−13.66	−3.94	0.00	−0.93	−0.44	−8.34
Ru	−0.22	6.84	8.81	−1.97	−7.06	−3.34	0.00	−0.09	−0.01	−3.62
Os	−1.76	6.74	11.82	−5.08	−8.50	−3.91	0.00	−0.06	−0.01	−4.52
Pu	3.08	18.66	22.11	−3.45	−15.58	−4.55	0.00	−1.10	−0.99	−8.94

[a] Results correspond to eq 3 and are given in eV.

Table 3. Energy Decomposition Analysis of $[M_2Br_8]^{2-}$ Complexes[a]

metal	E_B	$E_P + E_E$	E_P	E_E	E_O	E_O (a_1)	E_O (a_2)	E_O (b_1)	E_O (b_2)	E_O (e)
Mo	−0.93	6.71	12.70	−5.99	−7.64	−2.94	−0.01	−0.06	−0.04	−4.58
W	−1.90	6.09	15.73	−9.64	−7.99	−3.04	−0.01	−0.06	−0.03	−4.86
U	0.02	11.75	10.96	0.79	−11.73	−3.35	0.00	−0.18	−0.03	−8.17
Tc	−0.05	7.58	12.03	−4.45	−7.63	−3.27	−0.01	−0.10	0.25	−4.50
Re	−1.42	7.32	15.75	−8.43	−8.74	−3.67	−0.01	−0.08	0.13	−5.11
Np	1.30	15.76	18.00	−2.24	−14.47	−4.15	0.00	−0.74	−0.83	−8.74
Ru	−0.24	6.71	8.44	−1.73	−6.95	−3.25	−0.01	−0.10	−0.01	−3.56
Os	−1.74	6.75	11.52	−4.77	−8.49	−3.89	−0.01	−0.08	−0.01	−4.51
Pu	3.22	19.52	22.78	−3.26	−16.31	−4.64	0.00	−1.09	−1.04	−9.54

[a] Results correspond to eq 3 and are given in eV.

have three ($n = 3$), four ($n = 4$), or five ($n = 5$) unpaired electrons. For the d-block systems, the resulting electronic configurations are $[(a_1\uparrow)(e\uparrow\uparrow)]$ (Mo, W), $[(a_1\uparrow)(e\uparrow\uparrow)(b_2\uparrow)]$ (Tc, Re), and $[(a_1\uparrow)(e\uparrow\uparrow)(b_2\uparrow\downarrow)]$ (Ru, Os), where the orbitals of a_1, e, and b_2 symmetry are associated with the $[d_{z2}]$, $[d_{xz}, d_{yz}]$, and $[d_{xy}]$ metal-based functions, respectively. In the f-block systems, the unpaired electrons reside in orbitals of a_1, e, b_1, and b_2 symmetry and predominant metal f character corresponding to $[f_{z3}]$ (a_1), $[f_{z2x}, f_{z2y}]$ and $[f_x, f_y]$ (e), $[f_z]$ (b_1), and $[f_{xyz}]$ (b_2) functions, leading to electronic configurations that can be represented as $[(a_1\uparrow)(e\uparrow\uparrow)]$ (U), $[(a_1\uparrow)(e\uparrow\uparrow)(b_2\uparrow)]$ (Np), and $[(a_1\uparrow)(e\uparrow\uparrow)(b_1\uparrow)(b_2\uparrow)]$ (Pu).

The results corresponding to the fragment and energy decomposition analyses of all $[M_2X_8]^{2-}$ complexes studied in the present work are summarized in Tables 2 and 3. In addition to the individual components in eq 1, values for a combined "Pauli-plus-electrostatic" ($E_P + E_E$) contribution and a decomposition of the orbital-mixing term using C_{4v} irreducible representations are included. The combined Pauli-electrostatic and the orbital-mixing contributions respectively represent measures of the fragment interaction before and after electronic relaxation through a self-consistent-field procedure has taken place, and can thus be described as "prerelaxation" and "postrelaxation" effects.

The total bonding energy results suggest that the metal−metal interactions are (relatively) strong in the Mo and 5d (W, Re, Os) complexes but significantly less favorable or even slightly unfavorable in the Tc, Ru, and U species. For the Np and Pu systems, these data indicate that the $[M_2X_8]^{2-}$ complexes should be considerably unstable relative to the $[MX_4]^-$ fragments.

The orbital-mixing (E_O) component of the total bonding energy is rather stronger in the actinide complexes, compared with the d-block analogues, but its magnitude is not sufficiently large to compensate for the highly destabilizing influence of the prerelaxation ($E_P + E_E$) effects, which is ultimately responsible for the instability of the Np and Pu systems and the (much) less favorable nature of the metal−metal interactions in the U complexes relative to the Mo, W, Re, and Os species.

Although the destabilizing nature of the prerelaxation contributions is a consequence of the dominant influence of the Pauli repulsion, the electrostatic term appears to be the primary reason for the unfavorable or weak metal−metal bonding in the 5f complexes. The electrostatic interactions are not sufficiently strong to counteract the Pauli repulsion, at least to a degree comparable with that observed in the Mo, W, Re, and Os species. The less favorable nature of the metal−metal interactions in the Tc and Ru complexes, compared with the Mo and 5d analogues, can also be traced to effects associated with the electrostatic term, but in the case of $[Ru_2Cl_8]^{2-}$ and $[Ru_2Br_8]^{2-}$, the relatively weaker orbital-mixing contribution must be taken into consideration as well.

Since the magnitude of all individual bonding energy components is affected by the metal−metal bond lengths, it is convenient to carry out an energy decomposition analysis of the $[M_2X_8]^{2-}$ complexes at a fixed metal−metal distance to gain further insight into the trends in metal−metal interactions. Table 4 provides a comparison of the bonding energy results for the $[M_2Cl_8]^{2-}$ systems, calculated using optimized values for all structural parameters except the metal−metal bond length, which was fixed at 225 pm.

The total bonding energy values exhibit either negligible or small changes with respect to those obtained at the optimized metal−metal distances, but the individual components are more sensitive to the changes in bond length, with the most notable case being the Pu species. In general, the results in Table 4 reinforce the observation that the electrostatic interactions seem to play the most significant

Table 4. Energy Decomposition Analysis of $[M_2Cl_8]^{2-}$ Complexes Calculated at a Fixed Metal−Metal Distance of 225 pm[a]

metal	E_B	$E_P + E_E$	E_P	E_E	E_O
Mo	−0.82	7.11	14.15	−7.04	−7.92
W	−1.73	7.45	20.40	−12.95	−9.18
U	0.17	14.50	16.01	−1.51	−14.33
Tc	0.12	6.54	10.25	−3.71	−6.42
Re	−1.39	7.03	15.59	−8.56	−8.41
Np	1.34	13.19	13.82	−0.63	−11.85
Ru	−0.19	6.29	7.70	−1.41	−6.48
Os	−1.76	6.83	12.03	−5.20	−8.59
Pu	3.58	12.12	11.89	0.23	−8.54

[a] Results correspond to eq 3 and are given in eV.

role in connection with the unfavorable nature of metal−metal bonding in the actinide complexes, as the Pauli repulsion is of comparable magnitude to that in the d-block systems, but the electrostatic term has a much less stabilizing or even slightly destabilizing character. As a consequence, there is a strong destabilization associated with the prerelaxation effects that cannot be counterbalanced by the stabilization derived from the orbital interactions, despite the rather large magnitude of these contributions.

3.1.2. Prerelaxation: Pauli Repulsion and Electrostatic Interactions. The Pauli repulsion arises from four-electron two-orbital interactions, and previous studies have revealed that general results and trends for the Pauli component of the total bonding energy show correlations with trends in occupied fragment orbital overlaps.[28] This observation applies to the M_2X_6 complexes described and analyzed in one of our previous publications[9] and is also valid for the $[M_2X_8]^{2-}$ systems considered in this work.

Within each individual group, the results for the Pauli term (Tables 2, 3, and 4) are of similar magnitude, either at the optimized metal−metal bond length or at the fixed distance of 225 pm. The exceptions are the Pu complexes at their equilibrium geometry, but the large values obtained in these cases are due to the extremely short Pu−Pu distances at the corresponding energy minima. Examination of the occupied fragment orbital overlaps at the fixed metal−metal distance of 225 pm indicates that, within a given group, the results are similar in magnitude and, in general, the greatest values are found for the W, Re, and Os complexes. Thus, correlations are observed between the trends in Pauli repulsion and orbital overlaps.

There are general similarities in the molecular orbital structure of the $[MX_4]^-$ fragments that may contribute to the similarities in the Pauli repulsion and orbital overlap trends across all groups and series. For example, a common pattern is observed in the composition and character of the fragment orbitals, with most of the fully occupied valence levels being ligand-based and characterized by relatively small contributions from metal atom orbitals, but with the highest-lying levels being predominantly metal-based and thus most relevant to metal−metal bonding.

However, there are also significant differences in the role played by the outer-core orbitals in the Pauli repulsion between the d-block and f-block species, as shown by the results in Table 5, which are a comparison of energy decomposition analyses carried out using frozen cores that either include or exclude the $(n-1)$s and $(n-1)$p orbitals. These calculations were performed on complexes of the 4d and 5f elements, employing "large-core" (M.4p and M.6p, respectively) and "small-core" (M.3d and M.5d, respectively) basis sets but were not possible on the W, Re, and Os complexes because of unavailability of the equivalent large-core basis sets for these elements.

Table 5. Comparison of Energy Decomposition Analyses of $[M_2X_8]^{2-}$ Complexes Using Basis Sets with Large (M.4p, M.6p) and Small (M.3d, M.5d) Cores[a]

ligand	metal	δE_B	δE_P	δE_E	δE_O
Cl	Mo	−0.17	−0.53	0.32	0.04
	U	−4.98	−5.35	−1.00	1.37
	Tc	−0.16	−0.56	0.35	0.05
	Np	−8.20	−11.08	0.57	2.31
	Ru	0.09	−0.29	0.19	0.19
	Pu	−12.73	−15.17	−0.45	2.89
Br	Mo	−0.17	−0.41	0.20	0.06
	U	−5.11	−6.63	−0.04	1.56
	Tc	−0.12	−0.41	0.20	0.09
	Np	−8.38	−11.04	0.30	2.36
	Ru	0.12	−0.17	0.08	0.21
	Pu	−12.87	−15.16	−0.63	2.92

[a] Results correspond to eq 3 and are given as the difference (δE in eV) between the "large-core" and "small-core" calculations.

Table 5 reveals that the incorporation of the $(n-1)$s and $(n-1)$p atomic orbitals into the frozen core has a markedly different effect on the U, Np, and Pu systems compared with the Mo, Tc, and Ru species. In the latter case, only minor changes are observed in each of the energy terms, and therefore, the primary source of the Pauli repulsion appears to lie in the interactions between the valence orbitals. For the actinide systems, although the changes affecting the electrostatic and orbital-mixing terms are relatively small, a rather large decrease in the magnitude of the Pauli repulsion is observed, thus suggesting that there are significant destabilizing contributions arising from the interactions involving the outer-core orbitals.

Investigations of chemical bonding in main group systems using the energy decomposition analysis have indicated that the electron density distribution along bond axes should be taken into account for the interpretation of electrostatic interaction results.[29] In our study of Mo, W, and U M_2X_6 complexes,[9] we found that the electrostatic interactions were, in general, weaker in the U species than in the d-block analogues. This was partly due to the fact that the U−U distances were longer than the Mo−Mo and W−W bond lengths, but the nature and properties of the high-lying a_1 orbitals in the MX_3 fragments were also found to play a role in explaining the electrostatic differences. We were therefore interested to establish if similar considerations are applicable to the $[M_2X_8]^{2-}$ systems considered in this work.

The results from the energy decomposition analysis carried out at the fixed metal−metal distance of 225 pm (Table 4) indicate that the electrostatic contribution is significantly less stabilizing in the actinide species relative to the d-block

(28) Bickelhaupt, F. M.; Bickelhaupt, F. *Chem.−Eur. J.* **1999**, *5*, 162.

(29) Lein, M.; Szabó, A.; Kovács, A.; Frenking, G. *Faraday Discuss.* **2003**, *124*, 365.

analogues, particularly in the case of the 5d elements, and for $[Pu_2Cl_8]^{2-}$, the electrostatic term is actually predicted to have a slightly destabilizing effect.

Although the occupied fragment orbital overlaps have similar values across all groups and series, for the overlaps involving the $6a_1$ orbital of the $[MX_4]^-$ fragments (which is the highest-lying level of a_1 symmetry and is predominantly metal-based in character), smaller values are observed for the actinide than the d-block species. Analogously to the case of the MX_3 fragments in the M_2X_6 complexes, the $6a_1$ orbitals of the $[MX_4]^-$ fragments consist primarily of metal d-type functions in the d-block species and metal f-type functions in the actinide systems. The d orbitals in the d-block element fragments appear to be more localized and extended along the metal−metal axis, compared with the f orbitals in the f-block fragments, and these characteristics should allow for more significant overlap between the electron density on a given fragment and the metal atom nucleus in the opposite fragment, thus leading to stronger attractive electrostatic interactions. The relatively weaker electrostatic stabilization predicted for the 4d complexes, relative to that of the 5d analogues, is consistent with the more contracted nature of the metal d orbitals in the former.

These observations regarding the electrostatic interaction results at the fixed metal−metal distance of 225 pm are also valid in the case of the energy decomposition analysis performed at the optimized geometry (Tables 2 and 3), as the general trends are unchanged, with the exception of the Pu complexes. This is, however, a rather special case due to the fact that the extremely short Pu−Pu bond length obtained at the energy minimum implies that, at 225 pm, the metal−metal interaction is significantly further removed from its equilibrium state than for any other species considered, and it is possible that this is the reason why the trends within the [Ru, Os, Pu] group are altered.

3.1.3. Postrelaxation: Orbital-Mixing Interactions. We noted in section 3.1.1 that, at the optimized metal−metal distances, the orbital-mixing component of the total bonding energy is of significantly greater magnitude in the actinide complexes compared with the d-block analogues. Further insight can be gained by decomposing the orbital interactions in terms of C_{4v} irreducible representations, as shown in Tables 2 and 3.

In C_{4v} symmetry, the major contributions to the orbital interactions between the $[MX_4]^-$ fragments are associated with the a_1 and e representations, which correspond to metal−metal σ and π bonding, respectively. The calculated values of the b_1 and b_2 components, which correspond to metal−metal δ bonding, are much smaller, whereas those of the a_2 component are negligible as there are no directly relevant orbital interactions between the metal atoms that transform as this irreducible representation.

The larger orbital-mixing term in the actinide complexes arises from stronger interactions of both σ and π types, with the difference between the relative a_1 and e contributions, in the f-block systems compared with the d-block species, being (much) more significant for the e component. As discussed in our study of Mo, W, and U M_2X_6 complexes,[9] a general rationale for these results may be found in the fact that the orbitals required for metal−metal σ and π bonding appear to be more extensively involved in metal−ligand bonding in the d-block complexes than in the f-block analogues and, consequently, the participation of these orbitals in metal−metal bonding is greater in the latter compared with the former.

In the d-block complexes, the metal orbitals of b_1 symmetry (d_{x2-y2}) do not contribute to the metal−metal interaction as the corresponding levels of bonding and antibonding character are evenly occupied. Consequently, the b_1 component of the orbital-mixing term has a negligibly small value, relative to the a_1 and e components. A similar observation applies to the interactions involving b_2 orbitals in the Mo, W, Ru, and Os species and b_1 and b_2 orbitals in $[U_2Cl_8]^{2-}$ and $[U_2Br_8]^{2-}$.

The metal−metal δ-type interactions of b_1 and b_2 symmetry possess bonding character in the actinide complexes, and this characteristic is reflected in the relatively significant values obtained for the b_1 and b_2 orbital-mixing terms in the case of the Pu systems, where the corresponding orbitals are fully occupied (Chart 2). Nevertheless, comparison of the results for the a_1, e, b_1, and b_2 terms suggests that δ-like bonding between the metal atoms is considerably weaker than σ-like and π-like bonding.

In the Np complexes, only two electrons can reside in the two primary metal−metal δ orbitals, leading to three possible occupation patterns, $[(b_1)^2(b_2)^0]$, $[(b_1)^0(b_2)^2]$, and $[(b_1)^1(b_2)^1]$. For comparative purposes, the configuration corresponding to a fully occupied b_2 level, which is equivalent to that observed in Tc and Re complexes, was chosen for the energy decomposition analysis. However, it should be noted that the calculations on the $[NpX_4]^-$ fragments could only be successfully carried out in the case where the single electron associated with the δ-like orbitals was "smeared" over the b_1 and b_2 levels. Consequently, both the b_1 and b_2 orbital-mixing terms exhibit relatively significant values, and the combined ($b_1 + b_2$) results may represent a more appropriate measure of the δ-bonding energetics.

As in the case of the Pu complexes, the combined b_1 and b_2 components of the orbital-mixing term in $[Np_2Cl_8]^{2-}$ and $[Np_2Br_8]^{2-}$, whereas small in comparison with those of the a_1 and e components, are nontrivial. However, in the Tc and Re species, the b_2 component has a positive magnitude, suggesting that metal−metal δ bonding may be, energetically, slightly unfavorable. Even though previous calculations have indicated that the Re−Re δ bonds should be considered weak interactions,[23,24] the positive value of the b_2 orbital-mixing term in the Tc and Re systems is, in principle, an unexpected result because an analysis of structural trends in the D_{4h} and D_{4d} complexes of the 4d and 5d elements in groups 6, 7, and 8 suggests that δ bonding makes a favorable contribution to the metal−metal interaction.[10] To test possible functional dependence effects, we have repeated the calculations associated with the energy decomposition analysis using a number of density functionals, but in all cases considered, no substantive changes to this result were obtained.

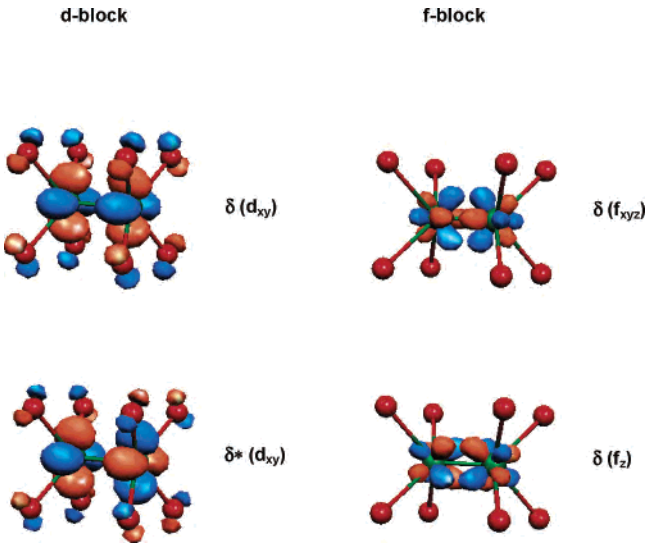

Figure 1. Spatial plots of the metal−metal δ-like molecular orbitals of $[M_2X_8]^{2-}$ complexes.

There are a number of differences in the nature of the metal−metal δ-like interactions in the Np and Pu complexes relative to the Tc and Re analogues, which may be connected with the differences observed in the results from the energy decomposition analysis. As shown in Figure 1, the directional properties of the δ-like orbitals on the individual metal atoms appear more favorable for metal−metal bonding in the f-block species compared with the d-block analogues, and this observation is consistent with the fact that the overlaps between the relevant (b_1 or b_2) $[MX_4]^-$ fragment orbitals are greater in magnitude in the Np and Pu systems than in the Tc and Re species. In addition and analogous to the case of the σ and π interactions, in the d-block complexes the metal d_{xy} orbitals, which are responsible for metal−metal δ bonding, are also significantly involved in metal−ligand bonding, whereas in the actinide systems metal−metal δ bonding is almost exclusively associated with interactions between the metal f_{xyz} and f_z orbitals. These play a smaller role in the interactions with the ligands, as the metal contributions to metal−ligand bonding are either of d character (predominantly) or of mixed d and f character. Examination of the energy levels in the Tc, Re, and Np complexes also indicates that the metal−metal δ-like orbitals of b_2 symmetry, which are the highest occupied molecular orbitals, are less destabilized with respect to the lower-lying levels in the Np species than the Tc and Re analogues.

3.1.4. Periodic Trends. Periodic trends in the energy decomposition analysis results for $[M_2Cl_8]^{2-}$ complexes across the 4d, 5d, and 5f series, derived from calculations carried out at a fixed metal−metal distance of 225 pm and at the optimized geometry, are shown in Figure 2.

Across the d-block series and at the fixed metal−metal distance of 225 pm, the Pauli repulsion and the electrostatic interaction terms exhibit a more significant variation than the orbital-mixing component and the total bonding energy. The approximately uniform weakening trends observed for the Pauli and electrostatic terms are consistent with the decrease in the magnitude of the (total and partial) orbital overlaps between the $[MX_4]^-$ fragments, which correlates with the expected contraction of the metal-based orbitals along the [Mo, Tc, Ru] and [W, Re, Os] directions.

The orbital-mixing interactions should also be affected by these factors, but in addition, the changes in the nature of the metal−metal interaction have to be considered. As found for the Pauli and electrostatic terms, the Mo and W complexes exhibit the strongest orbital-mixing interactions in the 4d and 5d series, respectively, mostly due to the influence of the contributions associated with the π-like interactions. However, the results for the Tc and Ru systems in the 4d series and for the Re and Os systems in the 5d series are largely similar as a consequence of opposing trends in the σ and π components and the slightly unfavorable character of the δ component in the Tc and Re species.

Examination of the results obtained at the optimized geometry of the d-block complexes, in comparison with those corresponding to the fixed metal−metal distance of 225 pm, reveals that the general trends exhibit relatively small changes, on a qualitative basis. Due to the fact that the optimized metal−metal bond lengths are longer than 225 pm for the Mo and W systems whereas those for the remaining 4d and 5d species are only slightly different or shorter than 225 pm, at their respective energy minima, the differences in the Pauli repulsion and electrostatic interaction values for $[Mo_2Cl_8]^{2-}$ compared with $[Tc_2Cl_8]^{2-}$ or $[Ru_2Cl_8]^{2-}$ and $[W_2Cl_8]^{2-}$ compared with $[Re_2Cl_8]^{2-}$ or $[Os_2Cl_8]^{2-}$ are (much) smaller. In the case of the orbital-mixing term, the largest values are found for the Tc and Re complexes, which are predicted to possess the shortest metal−metal distances in the 4d and 5d series, respectively.

In the case of the actinide complexes and unlike the d-block systems, the trends in the results obtained at the optimized geometry display opposite patterns to those derived from the calculations performed at the fixed metal−metal distance of 225 pm, and this observation applies to all individual components of the total bonding energy.

A factor that appears to have a significant influence on the noticeably different nature of the trends across the d-block and f-block series is the fact that the metal−metal distances span a considerably greater range in the case of the actinide complexes, approximately 27 pm compared with 10−11 pm for the 4d and 5d analogues. At the fixed bond length of 225 pm, the weakening trends in the Pauli, electrostatic, and orbital-mixing terms are consistent with the diminishing magnitude of the (total and partial) orbital overlaps between the $[MX_4]^-$ fragments and the expected contraction of the metal-based orbitals along the (U, Np, Pu) direction. However, at the energy minima, the considerably shorter metal−metal distance in $[Pu_2Cl_8]^{2-}$ and, to a smaller degree, $[Np_2Cl_8]^{2-}$ than in $[U_2Cl_8]^{2-}$ leads to a (significant) strengthening of the Pauli repulsion, electrostatic interactions, and orbital-mixing effects in the Np and, particularly, Pu complexes relative to the U species. A possible explanation for the considerable shortening of the bond lengths across the 5f block may be given in terms of a relatively rapid contraction of the metal-based orbitals and its effect on the

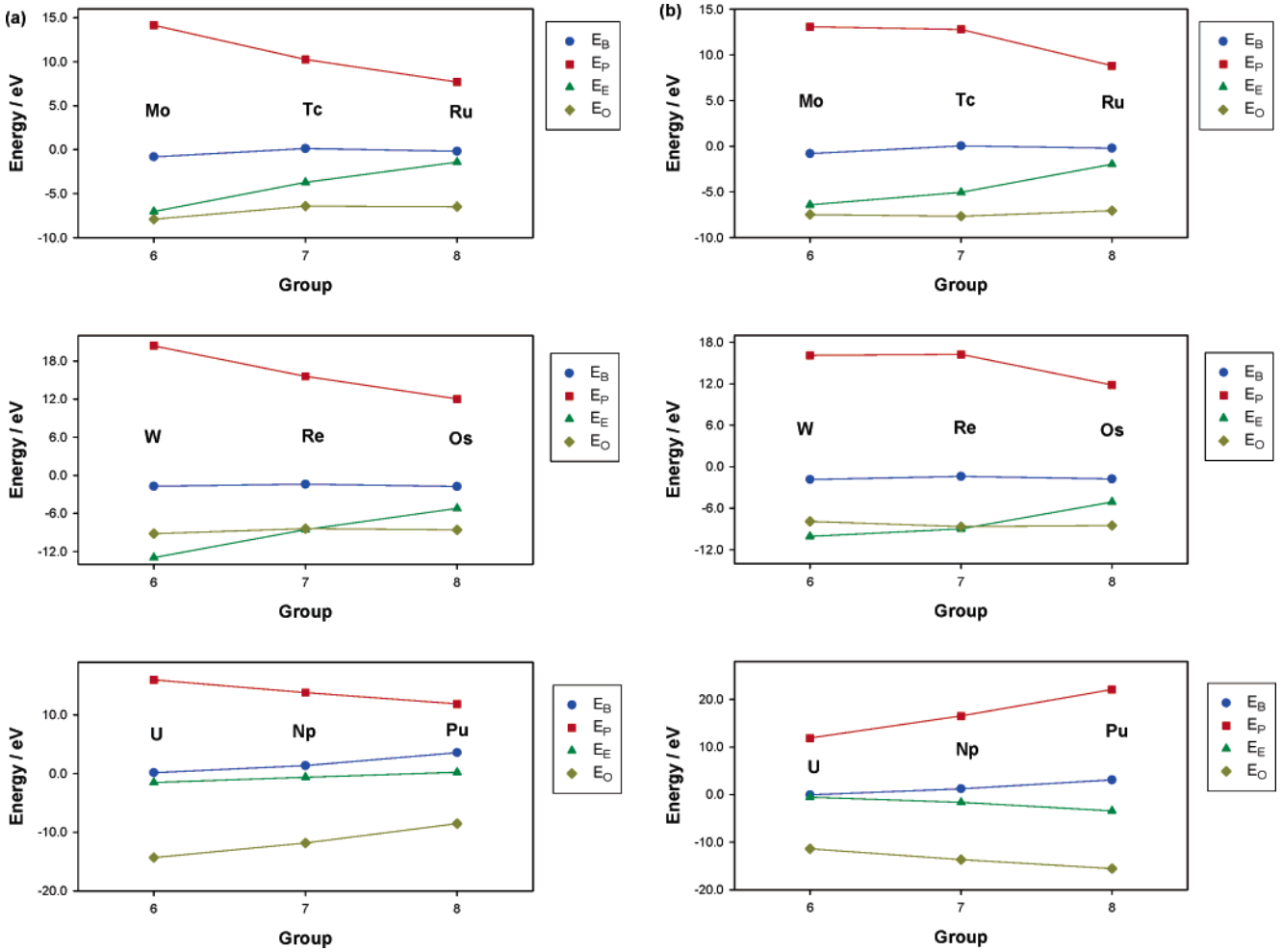

Figure 2. Periodic trends in the energy decomposition analysis results (E_B = total bonding energy, E_P = Pauli repulsion, E_E = electrostatic interaction, E_O = orbital mixing) for $[M_2Cl_8]^{2-}$ complexes across the 4d, 5d, and 5f series. Results correspond to calculations at (a) a fixed metal−metal distance of 225 pm and (b) the optimized geometry.

orbital overlaps, as significantly reduced metal−metal distances might then be required to achieve the optimum interplay between the bonding energy components.

4. Conclusion

A detailed analysis of the metal−metal interactions in a series of $[M_2X_8]^{2-}$ (X = Cl, Br) complexes involving 5f (U, Np, Pu), 5d (W, Re, Os), and 4d (Mo, Tc, Ru) elements has been carried out using an energy decomposition approach. The strongest metal−metal interactions are predicted for the W, Re, Os, and, to a smaller degree, Mo complexes, with metal−metal bonding in the Tc, Ru, and U species being significantly less favorable or even slightly unfavorable. For the Np and Pu systems, the energy decomposition analysis suggests that the $[M_2X_8]^{2-}$ complexes should be considerably unstable relative to the $[MX_4]^-$ fragments.

The relatively weak or unfavorable nature of metal−metal bonding in the actinide complexes is a consequence of the significantly more destabilizing character of the "prerelaxation" Pauli-plus-electrostatic effects in the interaction between the $[MX_4]^-$ fragments, and a comparatively weak electrostatic contribution appears primarily responsible for this result. The "postrelaxation" fragment interactions, associated with orbital-mixing effects, are, however, stronger in the U, Np, and Pu complexes than in the d-block analogues. Thus, the general results and trends are similar to those obtained in our study of Mo, W, and U M_2X_6 species and support the observation that the energy decomposition analysis of actinide−actinide bonds suggests that there are intrinsic intramolecular reasons as to why metal−metal bonding is so scarce in the 5f block.

The periodic trends in the energy decomposition analysis results for $[M_2Cl_8]^{2-}$ complexes, derived from calculations carried out at the optimized geometries and at a fixed metal−metal distance of 225 pm, show greater variation in the general behavior and some particular properties across the actinide series than in the d-block series. As noted in the introduction, crossing the early-to-middle part of the 5f series, one sees that the radial extension of the 5f orbitals is reduced more rapidly than that of the d orbitals in corresponding transition metal series as the chemistry of the actinides begins its trend toward more lanthanide-like behavior. It is therefore not unreasonable to expect more significant changes in chemical behavior and properties across the (U, Np, Pu) series than across d-block series involving elements from groups 6, 7, and 8.

Acknowledgment. We are grateful for financial support from the Engineering and Physical Sciences Research Council (under Grant No. EP/C533054) and for allocation of supercomputer time from the National Service for Computational Chemistry Software.

IC0623260